NASA TECHNICAL NOTE

EFFECTS OF SILICON ADDITIONS ON OXIDATION AND MECHANICAL BEHAVIOR OF THE NICKEL-BASE SUPERALLOY B-1900

Robert V. Miner, Jr., and Carl E. Lowell

Lewis Research Center
Cleveland, Ohio 44135

NATIONAL AERONAUTICS AND SPACE ADMINISTRATION • WASHINGTON, D. C. • JUNE 1975

1. Report No.	2. Government Accession No.	3. Recipient's Catalog No.
NASA TN-D-7989		

4. Title and Subtitle
EFFECTS OF SILICON ADDITIONS ON OXIDATION AND MECHANICAL BEHAVIOR OF THE NICKEL-BASE SUPERALLOY B-1900

5. Report Date
June 1975

6. Performing Organization Code

7. Author(s)
Robert V. Miner, Jr., and Carl E. Lowell

8. Performing Organization Report No.
E-8248

9. Performing Organization Name and Address
Lewis Research Center
National Aeronautics and Space Administration
Cleveland, Ohio 44135

10. Work Unit No.
505-01

11. Contract or Grant No.

12. Sponsoring Agency Name and Address
National Aeronautics and Space Administration
Washington, D.C. 20546

13. Type of Report and Period Covered
Technical Note

14. Sponsoring Agency Code

15. Supplementary Notes

16. Abstract

Cast B-1900 test specimens with nominal additions of 0-, 0.5-, and 1-wt % Si were tested in oxidation, thermal fatigue, sulfidation, tension, and stress rupture and were also extensively studied metallographically. Alloy B-1900 modified with 0.6- or 1.2-wt % Si exhibited oxidation resistance equivalent to that of aluminide-coated B-1900 during cyclic, high-gas-velocity oxidation tests. Resistances to thermal fatigue and sulfidation were improved by the Si additions, but aluminide-coated B-1900 is definitely superior in both respects. Stress-rupture tests at 1000° C of specimens given the standard heat treatment to simulate an aluminide coating cycle showed Si to be detrimental. However, application of another heat treatment increased the rupture life of the alloy with 0.6-wt % Si to that of the unmodified B-1900 given the standard heat treatment.

17. Key Words (Suggested by Author(s))	18. Distribution Statement
Superalloy; High-temperature alloy; Oxidation; Mechanical properties; Corrosion	Unclassified - unlimited STAR Category 26(rev.)

19. Security Classif. (of this report)	20. Security Classif. (of this page)	21. No. of Pages	22. Price*
Unclassified	Unclassified	31	$3.75

* For sale by the National Technical Information Service, Springfield, Virginia 22151

EFFECTS OF SILICON ADDITIONS ON OXIDATION AND MECHANICAL BEHAVIOR OF THE NICKEL-BASE SUPERALLOY B-1900

by Robert V. Miner, Jr., and Carl E. Lowell

Lewis Research Center

SUMMARY

Previous studies at this laboratory showed that small silicon additions greatly improved the oxidation resistance of Ni_3Al (gamma prime) and a high-fraction-gamma-prime superalloy, B-1900. The present work was done to confirm the improved oxidation resistance of B-1900 with silicon added in high-gas-velocity tests and to evaluate its behavior in sulfidation, tensile, and stress-rupture tests.

Alloy B-1900 modified with 0.6- or 1.3-wt% silicon exhibited oxidation resistance equivalent to that of aluminide-coated B-1900 during cyclic heating to 1100° C in a Mach 1 burner exhaust. Resistance of B-1900 to thermal fatigue cracking in this test was improved by the addition of silicon, but resistance of the aluminide-coated B-1900 was definitely superior.

Sulfidation tests at 900° C in the burner facility also showed an improvement due to the silicon additions, but aluminide-coated B-1900 showed much less attack.

Stress-rupture testing of the alloys given the standard heat treatment to simulate the aluminide coating cycle, 1080° C for 4 hours plus 900° C for 10 hours, showed the silicon additions to have produced a considerable reduction in 1000° C rupture life. It was possible, however, to increase the 1000° C rupture life of all the alloys by employing high-temperature solution treatments. After a heat treatment of 1200° C for 4 hours plus 900° C for 10 hours, B-1900 with 0.6-wt% silicon had a 1000° C rupture life equivalent to that of B-1900 given the standard heat treatment. However, the life of B-1900 with 1.1-wt% silicon could not be increased to this level.

The effect of silicon on high-temperature rupture life can be explained by marked changes in microstructure. Silicon causes more gamma prime to be precipitated as massive nodules during solidification rather than from the matrix on subsequent cooling. A Laves phase, essentially $Mo(Ni,Si)_2$, was also promoted by the silicon additions. The heat treatments which improved rupture properties provided some refinement of the gamma-prime distribution.

INTRODUCTION

The present investigation of the effects of silicon additions to the complex nickel-base superalloy B-1900 stems from earlier studies at this laboratory. These studies of the oxidation behavior of simple alloys were intended to show the effects of some individual elements on the major phases in nickel-base superalloys and their oxidation-resistant coatings (refs. 1 and 2). The effects of three elements which form very stable oxides, silicon (Si), chromium (Cr), and titanium (Ti), were studied in three phases in the nickel-aluminum (Ni-Al) system: (1) gamma (the Ni-rich solid solution); (2) gamma prime (Ni_3Al), which is the basis of the major strengthening phase in Ni-base superalloys; and (3) beta (NiAl), which is the basis of aluminide coatings. A great improvement in the oxidation resistance of the gamma-prime phase was produced by the replacement of 1- or 3-at.% Al with equal quantities of Si. The alloy Ni-24Al-1Si (at.%) was as oxidation resistant as the beta phase (NiAl).

Based on these promising results a study was undertaken to determine if Si additions would also provide large improvements in the oxidation resistance of a superalloy with a high fraction of gamma prime. Alloy B-1900, a currently used turbine blade alloy, was chosen as the basis for this study (ref. 3). It contains about 60-vol% gamma prime. The addition of 1-wt% Si to B-1900 resulted in a marked improvement in oxidation resistance. During thermal cycling from room temperature to either 1100° or 1200° C in static air, the B-1900 + 1-wt% Si samples were still increasing in weight at a low steady rate. Under these conditions the oxide scale on the B-1900 samples spalled severely, producing a rapidly increasing rate of weight loss.

In the present investigation the resistance of the B-1900 + 1-wt% Si alloy to cyclic oxidation in high-velocity gas and its mechanical properties were studied to learn if it might be suitable for turbine blades without requiring a coating for additional oxidation protection. An alloy not requiring a coating might, besides providing an opportunity for cost savings, be more reliable in terms of oxidation resistance. A less oxidation-resistant alloy protected by a coating may still suffer local damage beneath any imperfections in the coating.

Cast B-1900 specimens with nominal additions of 0-, 0.5-, and 1.0-wt% Si were obtained from a commercial vendor of castings for turbine engines. An alloy with 0.5-wt% Si (1-at.% Si) was obtained, as well as an alloy with 1-wt% Si (2-at.% Si) as tested previously in oxidation (ref. 3). Addition of 1-at.% Si had previously been shown as effective as 3-at.% Si in improving the oxidation resistance of Ni_3Al (refs. 1 and 2). And it was expected that the lower Si concentration of 1 at.% in the B-1900 modification might be less detrimental to mechanical properties. Although the exact reason is not apparent in the literature, it is known that maximum Si concentrations of about 0.2 wt% are generally specified for advanced cast Ni-base superalloys.

The alloys were evaluated in oxidation, including cyclic oxidation testing at 1100° C in a Mach 1 burner exhaust to simulate engine conditions. Sulfidation resistance was evaluated in the same burner facility with synthetic sea salt injected into the burner. In these tests, B-1900 specimens with a commercial aluminide coating were run for comparison. Since the temperature was cycled in the 1100° C burner facility oxidation test, it was also a very severe thermal fatigue test. Other mechanical testing, tensile and stress-rupture, was performed on the alloys that had been given various heat treatments. And, finally, the effects of Si on the microstructure of B-1900 were determined by extensive microscopic, X-ray diffraction, and chemical analyses.

MATERIALS AND PROCEDURES

Materials

Alloy B-1900 and two modifications containing nominally 0.5- and 1.0-wt % Si were cast by an aircraft gas turbine engine manufacturer's approved vendor of B-1900 castings. Each alloy was cast into clusters of mechanical test bars and clusters of static-air oxidation specimens and high-gas-velocity oxidation specimens. It was intended that all specimens be cast from the one master heat qualified by the engine manufacturer, with Si additions added during remelting to make the modified alloys. However, due to mold breakage during casting, the desired number of mechanical test bars was not obtained. Since no more of the first master heat remained, a second qualified master heat was used to make more mechanical test bars of each nominal composition.

The vendor's analyses of the two master heats are presented in table I together with the nominal composition of B-1900 (ref. 4). The vendor's analyses for Si concentration in each casting are given in table II. All are close to aim except for castings 1-0 and 1-6. Note that the static-air and high-gas-velocity oxidation specimens for each composition were cast in the same cluster mold.

All the mechanical test specimens were examined by fluorescent dye penetrant, and a few were etched for grain-size determination. Silicon did not affect the grain size of the castings. Grain sizes ranged from 0.8 to 1.5 mm.

Heat Treatment

Some mechanical test specimens and all oxidation test specimens were given the standard heat treatment which is employed by the principal user of B-1900 to simulate the effect of an aluminide coating diffusion cycle and subsequent aging treatment when evaluating castings (private communication from S. S. Blecherman, Pratt & Whitney

Aircraft). This consists of 4 hours at 1080° C, followed by an air cool, and then aging for 10 hours at 900° C. The other mechanical test specimens were heat treated by using higher temperatures for the initial treatment and the same aging treatment of 10 hours at 900° C. These heat treatments are identified, together with the resultant mechanical properties, in the section RESULTS AND DISCUSSION.

Static-Air Oxidation Tests

Isothermal. - Cast bars of the three alloys, about 10.2 cm by 2.5 cm by 0.6 cm, were cut into specimens about 1.3 cm by 2.5 cm by 0.6 cm. A 0.25-cm hole was drilled in each specimen for a thin quartz suspension rod. All surfaces were glass-bead blasted, and immediately before testing the specimens were cleaned ultrasonically in trichloroethylene.

Isothermal oxidation tests were performed at 1100° and 1200° C in static air for 100 hours. The apparatus used is described in reference 1. A continuous-recording electrobalance was used to measure weight change of the oxidizing specimens to a precision of ±0.1 mg. Above the hot zone of the furnace a platinum wire connected the quartz suspension rod to the balance. The temperature was continuously monitored and found to be constant to ±2° C.

After the tests the oxides on the specimens and their spalls were identified by X-ray diffraction. Actual use temperatures for B-1900 are probably no higher than about 1000° C. However, in testing at 1100° C the accelerated oxidation allows differences among alloys to become observable in a practical length of time. The ranking of the alloys should be basically the same as for testing at 1000° C.

A few specimens of the alloys were oxidized isothermally for short times in a furnace and studied by electron diffraction in an attempt to determine any effects of Si on the initial stage of oxidation.

Cyclic. - The apparatus used to study oxidation during cyclic heating in static air is fully described in reference 5 and briefly here. A multitube furnace allowed testing of six specimens simultaneously. Samples were automatically cycled in and out of the furnace by means of a pneumatic cylinder controlled by timers operating solenoid valves. The apparatus was used with spall collector cups automatically positioned under the samples during the cooling portions of the cycles. At the conclusion of the test the samples were weighed to determine weight change, and the spalled and in-situ oxides were analyzed by X-ray diffraction.

Specimens were cycled between 1100° C and approximately room temperature for total heating times of 200 hours. A variety of cycles were used, as shown in table III. Heating and cooling curves for a typical sample are shown in figure 1.

High-Gas-Velocity Oxidation Tests

High-gas-velocity oxidation was studied by cyclically heating specimens to 1100° C in a Mach 1 burner exhaust and then cooling them to near room temperature in a Mach 1 cool-air stream. Jet A fuel was used in the burner. The cycle consisted of 1 hour of heating and 3 minutes of cooling. The specimens reached temperature on heating in about 1 minute. Tests were run to a total of 300 hours of heating time.

The test apparatus and specimen configuration are completely described in reference 6 and only briefly herein. Eight specimens can be fitted into a specimen holder, which is rotated at 900 rpm to maintain the same temperature for all the specimens. The specimens are automatically cycled from burner exhaust to cool-air stream. The temperature of the specimens when in the burner exhaust can be controlled to ±15° C.

The specimen configuration is 0.64 cm by 2.54 cm by 10.16 cm and has flat parallel sides except for a tapered leading edge. This configuration and localized heating in the center of the specimen make the test a severe one for thermal-fatigue resistance as well as for oxidation resistance. For estimation of specific weight loss an effective specimen surface area of 30 cm^2 is assumed (ref. 6).

Besides the specimens cast for this program, aluminide-coated B-1900 specimens were tested for comparison. All the specimens were cast to size. The bare specimens were glass-bead blasted, and then all were cleaned ultrasonically in trichloroethylene before testing. They were weighed at the beginning of the test and were subsequently removed from the apparatus at 20-cycle intervals to be weighed and visually inspected for thermal fatigue cracking. At the conclusion of the test the oxides formed were analyzed in situ by X-ray diffraction. And finally, the specimens were sectioned for microscopic examination.

Another set of specimens was tested for resistance to hot corrosion. A concentration of 5-ppm, ASTM specification D-1141-52, Formula A synthetic sea salt was used in the burner exhaust. The specimens were cycled to 900° C for 200 hours of total heating time. Otherwise, the test was conducted as previously described for the high-gas-velocity oxidation tests.

Mechanical Testing

The specimens for tensile and stress-rupture testing had 0.6-cm diameter and 3.2-cm gage length. All tests were performed in air and in accordance with ASTM recommended practice. Elongation was determined by dividing the specimen elongation measured from punchmarks on the specimen shoulders by the length of the reduced section.

Metallography and Phase Analyses

Metallographic examination was performed on all alloys after the various heat treatments employed. The etchant used was 33 parts each of nitric acid, acetic acid, and water plus 1 part of hydrofluoric acid. Quantitative electrolytic phase extractions were performed by the methods of reference 7 on alloy samples given the standard heat treatment and also on samples additionally exposed for 1500 hours at 870° C to test their phase stabilities. The phases present in the extracted residues were determined by X-ray diffraction. The gamma-prime phases extracted from alloy samples given the standard heat treatment were also chemically analyzed by the methods of reference 8. The compositions of some individual phases were also determined qualitatively in situ by electron microprobe and by energy dispersive spectroscopy.

RESULTS AND DISCUSSION

Static-Air Oxidation Tests

Isothermal. - The results of the 100-hour isothermal oxidation tests are shown in figure 2. Parabolic oxidation kinetics were not observed and were not expected for such complex alloys. At 1200° C the effect of Si concentration was obvious. As Si concentration increased, the oxidation rate decreased. This trend also appears in the 1100° C data, but the differences among the curves are not much greater than the scatter usually observed for this test.

The oxides found on these specimens and in their spalls were the same as those found by Garlick and Lowell (ref. 9): Al_2O_3, spinels, tapiolite, and NiO on some specimens. The only differences among the alloys were a higher fraction of Al_2O_3 and less spinels and NiO with increased Si concentration in the alloys.

Reflection electron diffraction studies of specimens oxidized for less than 1 minute at 1200° C showed no obvious differences among the initial oxides formed on the three alloys. The oxides found on these specimens were essentially the same as those on the specimens oxidized for 100 hours except that Cr_2O_3 was also found and Al_2O_3 was not identified. Thus, many oxides are present even in the earliest stages of oxidation.

The effect of Si on the oxidation behavior of Al_2O_3-forming Ni-base alloys has received some prior study at this laboratory (refs. 1 to 3). However, its effect on Cr_2O_3-forming, Ni-20Cr alloys has received considerable study (refs. 10 to 14). The addition of Si to Ni-20Cr greatly improved its oxidation resistance. The following mechanisms have been proposed to explain this effect:

(1) Si promotes keying of the oxide scale into the base metal and thus improves resistance to spalling.

(2) The SiO_2 which forms at the metal-oxide interface retards metal ion diffusion to the surface, though the SiO_2 may be amorphous when formed at temperatures of 1100° C and below. (Crystalline SiO_2 has never been observed in the present study.)

The view of the effect of Si on Cr_2O_3-forming alloys taken by one of the authors (ref. 13) does not support either of these mechanisms. This view is also felt to apply generally to the effect of Si in B-1900, although it is an Al_2O_3-forming alloy, and is summarized here. The electron diffraction studies previously referred to lend support to the view that many oxides are nucleated locally in the initial stages of oxidation, not just the oxide that would be predicted thermodynamically from the bulk composition of the alloy (refs. 15 and 16). The later composition of the scale is then determined by the kinetics of the many reactions involved. The role of Si in this process appears to be to reduce the rate of NiO formation on Ni-base alloys. Since NiO formation competes with that of the sesquioxides, Si additions allow more complete coverage by the more protective sesquioxides on Ni-Cr and Ni-Al alloys and thus lower oxidation rates.

Reduced rates of NiO formation attributed to Si additions have been observed for Cr_2O_3-forming Ni-20Cr alloys (ref. 13) and for alloys forming only NiO (ref. 17). The present study and the work on Ni-20Cr alloys also show a reduction in spinels in the scales (formed by solid-state reaction of NiO and the sesquioxide).

It is true, in general, that alloys with lower isothermal oxidation rates (i.e., which form thinner scales) are more resistant to spalling during cyclic oxidation (ref. 18). Indeed, the results reported in the following sections show that the Si additions were very beneficial to cyclic oxidation resistance.

Cyclic. - The results of the cyclic oxidation tests in static air are shown in figure 3. The weight changes shown were determined after 200 hours of total heating time for cycle periods of 100, 10, 1, and 0.1 hours. The specimens were heated to 1100° C. The data show that the alloys with Si added have markedly improved resistance to cyclic oxidation compared with the unmodified B-1900. Alloy B-1900 shows a regular increase in weight loss due to oxide spalling with increasing cycle frequency (decreasing period). The alloys with Si added show no significant change. However, the alloy with 1.3-wt% Si does appear to be slightly improved with respect to the 0.6-wt%-Si alloy.

High-Gas-Velocity Oxidation and Hot Corrosion Tests

In order to more closely simulate gas turbine engine service conditions, Mach 1 burner facility testing was performed. For comparison, B-1900 specimens with a commercial aluminide coating were tested at the same time. The specimens were cycled between 1100° C and ambient temperature with 1-hour heating and 3-minute cooling periods for a total of 300 hours of heating. The results are shown in figure 4. In brief, B-1900 with 0.6- or 1.3-wt% Si showed markedly improved high-gas-velocity oxidation

resistance relative to the unmodified B-1900 and had the same oxidation resistance as the aluminide-coated specimens.

Increasing Si concentration provided some improvement in thermal-fatigue resistance, but neither of the Si-modified alloys were as effective in this respect as the aluminide-coated B-1900, which never cracked in these tests. Cracks were first observed on the B-1900 + 1.3-wt%-Si specimens at 100 cycles. The B-1900 and B-1900 + 0 6-wt%-Si specimens were cracked at 60 cycles. But cracking was less extensive in the B-1900 + 0.6-wt%-Si specimens at the end of the test and still less extensive in the B-1900 + 1.3-wt%-Si specimens.

After testing, the burner facility samples were sectioned and examined metallographically. Figure 5 shows the microstructure of B-1900 and B-1900 + 1.3-wt%-Si specimens after the 300-hour test. Both specimens show the usual Al depletion zone (e.g., see ref. 19), but it is about 50 percent thicker in the unmodified B-1900.

Sulfidation tests were performed in the same burner facility used for the oxidation tests with 5-ppm sea salt injected into the burner. The cycle was the same as for the oxidation tests except that the specimens were heated to 900° C, which is in the temperature regime where sulfidation attack of B-1900 is most severe according to Walters (ref. 20).

The weight change data in figure 6 show that Si does increase the sulfidation resistance of B-1900 but that the aluminide-coated B-1900 clearly has the best resistance. No attempt was made to estimate specific weight losses (mg/cm^2) because the area of attack was very irregular. Also, the most severe attack did not occur in the 900° C hot zone as expected from Walters' data, but in the lower temperature areas of the specimens. At least two explanations are possible: (1) the hot-zone temperature was somewhat above the approximately 950° C upper limit for attack reported by Walters, or (2) the upper temperature limit for attack is actually somewhat lower than 900° C.

Mechanical Properties After Standard Heat Treatment

Stress rupture. - Specimens of each casting were given the standard heat treatment consisting of 1080° C for 4 hours, to simulate an aluminide coating diffusion cycle, followed by an aging treatment of 900° C for 10 hours. Specimens were tested in stress rupture at 1000° C and 152 MN/m^2 and in tension at room temperature and 650° C.

The stress-rupture lives at 1000° C and 152 MN/m^2 for specimens from all the castings given the standard heat treatment are presented in table IV. The average lives of the castings are shown as a function of Si concentration in figure 7. The effect of Si is seen to be deleterious and very much the same in both master heats. The effect of 1.0-wt% Si is indicated to be about a 60 percent reduction in rupture life. This would correspond to an approximate 20° C decrease in allowable use temperature. A reduction

of about 20 percent in rupture life, or about a 5^{o} C decrease in use temperature, is indicated for 0.5-wt % Si.

It will be shown, however, that another heat treatment can be applied which increases the rupture life of the alloy with 0.6-wt % Si, made from the second master heat, to nearly that of unmodified B-1900 given the standard heat treatment.

Data for rupture elongation and reduction of area are also presented in table IV. Silicon is seen to have no marked effect on rupture elongation or reduction of area.

"Typical" data for cast-to-size test bars of B-1900 given the standard heat treatment (private communication from S. S. Blecherman, Pratt & Whitney Aircraft) are given for all the mechanical property tests conducted in this program (tables IV and V). It can be seen that the properties of the specimens of all the alloys cast for this program, including the two master heats without Si added, are somewhat low compared to the typical data.

Tensile. - Single specimens of each alloys cast from the first master heat and given the standard heat treatment were tested in tension at room temperature and at 650^{o} C, about the temperature at which B-1900 exhibits greatest tensile strength. The data are presented in table V and are shown as a function of Si concentration in figures 8 and 9.

Silicon does not have a great effect on yield or ultimate tensile strength at room temperature or 650^{o} C.

For example, the ultimate tensile strength of B-1900 with 0.8-wt % Si was decreased about 7 percent at room temperature and 9 percent at 650^{o} C. But with 1.0-wt % Si, ultimate tensile strength was not decreased at either temperature. The yield strength of B-1900 with 1.0-wt % Si was decreased at room temperature, about 9 percent, but not at 650^{o} C.

Ductility decreased with the addition of Si, particularly at 650^{o} C. The alloys with 0.8- and 1.0-wt % Si had 1.0 and 1.5 percent elongations as compared with about 2.8 and 6.3 percent for the specimens from the two castings of the base alloy. B-1900 typically has 5 percent elongation at 650^{o} C.

The tensile properties of all three alloys given the standard heat treatment, including B-1900 without Si added, were lower then typical values for B-1900 given the same heat treatment. Typical properties are presented in table V for comparison.

Effects of Heat Treatment on Rupture Life

As is discussed in the next section, Metallography and Phase Analyses, the primary effect of Si on the microstructure of B-1900 is to increase the degree of segregation during solidification. This leads to the formation of large eutectic gamma-prime nodules at grain boundaries and in the interdentritic regions and reduced volume fraction of fine gamma-prime precipitated in the matrix. In an attempt to dissolve the large

gamma-prime nodules and reprecipitate them in a finer form, specimens were given high-temperature solution treatments followed by the standard aging at 900° C for 10 hours. These specimens were then tested in stress rupture.

Figure 10 shows the average rupture lives at 1000° C and 152 MN/m^2 as a function of Si concentration for the alloys prepared from the second master heat and given four different heat treatments. Reduction in area is shown in figure 11 to indicate the effect of Si on ductility. Elongations could not be measured on the specimens from casting 2-3 given the standard heat treatment because of accidental damage during removal from the test grips. All the rupture data are presented in table IV. The solution treatments employed were 1200° C for 2 hours, 1230° C for 24 hours, and 1260° C for 24 hours. Data for the specimens given the standard coating cycle and aging heat treatment are also shown in figures 10 and 11 for comparison.

The most successful of the heat treatments was the 1200° C/2 hr solution treatment. The average rupture life of the alloy with 0.6-wt% Si was 73.0 hours, as compared with 54.8 hours for this alloy given the standard coating cycle simulation. The 73.0-hour average life is very nearly that of the alloy without Si added given the standard heat treatment. The 1200° C-solution-plus-aging treatment improved the rupture life of all three alloys, but even so the average life of the 1.1-wt%-Si alloy was only 39.9 hours. None of the heat treatments used increased the life of the 1.1-wt% Si alloy to near that of the alloy without Si added and given the standard heat treatment.

The higher solution temperatures of 1230° and 1260° C did not improve rupture properties over those for the 1200° C solution treatment for the alloys with Si added. Ductility was substantially reduced after these higher heat treatments for the 0.6-wt%-Si alloy as well as for unmodified B-1900.

Both the 1200° C/2 hr and 1230° C/24 hr solution treatments improved the ductility of the 1.1-wt%-Si alloy, even though there was a possible indication of incipient melting at 1230° C. Definite incipient melting, however, occurred at 1260° C, and this may have caused the great reduction in ductility in the 1.1-wt%-Si alloy shown in figure 11.

At the completion of the heat treatment study just described a few specimens remained, some of those prepared from the first master heat. These specimens were given the 1200° C/2 hr solution treatment plus the 900° C aging and then tested in stress-rupture at 760° C and 648 MN/m^2.

The effects of Si concentration on rupture life at these test conditions are difficult to assess because of the large scatter in the data for the specimens without Si added. On the basis of average life - 49.9, 16.8, and 35.0 hours for the base, and 0.8- and 1.1-wt%-Si alloys, respectively, there appears to be a minimum in rupture life as a function of Si concentration. Similar results were shown for tensile strength at room temperature and 650° C for these same alloys given the standard heat treatment. However, two of the three specimens of the base alloy had short lives, 29.3 and 12.1 hours; thus, based on these limited data, it cannot be stated with confidence that Si has reduced

rupture life. It does appear, though, that the Si additions have lowered the reduction of area. Elongation, which was low even for the base alloy specimens (2.1 percent), was not greatly affected by the Si additions.

Metallography and Phase Analyses

Standard heat treatment. - The addition of small amounts of Si to B-1900 has a marked effect on its microstructure. The primary changes are an increase in the amount of massive gamma-prime nodules formed during solidification and the formation of a $Mo(Ni,Si)_2$ Laves phase, both of which could be responsible for the decrease in stress-rupture life.

Shown in figures 12 to 14 are secondary electron photomicrographs of unmodified B-1900 and B-1900 with 0.6- and 1.3-wt% Si, respectively. They are from castings 1-4, 1-5, and 1-6, which have been given the coating cycle heat treatment.

Most apparent in these micrographs is the great increase in the amount of massive gamma-prime nodules with increasing Si concentration. These are the dark grey masses present in the interdendritic areas and at grain boundaries. There is a small volume fraction of these in the B-1900 specimen, though none is visible in figure 12.

The increase in gamma-prime nodules and the Laves phase formation are due to increased segregation during solidification. Sittner (ref. 21) discusses segregation caused by ternary Si additions to binary alloys of Ni with Co, Cr, and Mo, respectively. Silicon is concentrated in the last liquid to solidify, while the second element of each ternary alloy is concentrated in the dendrite centers. The degree of segregation of the second element decreases in the order Co, Cr, and Mo. The increased coring due to Si can be readily seen by comparing figures 12 and 14.

It was attempted to determine the amounts of the minor phases and gamma prime in castings 2-1, 2-2, and 2-3 by the electrolytic extraction methods of reference 7 and also to determine the composition of the gamma prime by analysis of the extracted residues. The results of these experiments are presented in table VI.

X-ray diffraction analyses of the alloys' minor phases, which were extracted by using the HCl-methanol electrolyte, revealed only an MC-type carbide in the unmodified B-1900 and a Laves phase as well as the carbide in the alloys with Si added. The MC in all three alloys had a lattice parameter of about 0.437 nm. Identification of the Laves phase in the alloys with Si added is discussed later in this section. Although there is probably an M_3B_2-type boride in the alloys (ref. 22), no diffraction lines not attributable to the MC or Laves phases were found.

The amounts of the minor phases were 1.5, 2.4, and 3.2 wt% in the nominal 0-, 0.5-, and 1-wt%-Si alloys, respectively. The increasing amount was probably due to the formation of the Laves phase, which was promoted by the Si additions.

The material extracted from the alloys by using the ammonium sulfate - citric acid electrolyte appeared to contain only the gamma-prime and MC phases. The decreasing amount of gamma prime plus MC as a function of increasing Si concentration in the alloys may well not indicate an actual decrease in the amount of gamma prime. It may merely mean poor recoveries in the extraction process because of the presence of the Laves phase in the alloys with Si added. Other work at this laboratory and elsewhere (ref. 7) has shown the recovery of gamma prime by this electrolytic extraction method to be low when intermetallics such as sigma, mu, and Laves are present in the alloy.

Thus, the effect of the Si additions on the total amount of gamma prime in the alloys could not be determined by the electrolytic extraction method. The fraction of gamma prime determined for the unmodified B-1900 should be valid, however, and does compare well with the value of Kriege and Baris (ref. 23).

The material extracted from the alloys by using the ammonium sulfate - citric acid electrolyte was chemically analyzed by emission spectroscopy for all the elements listed in table VI except Si. Atomic absorption spectroscopy was used to determine Si by the method of known additions. The bulk alloys were also analyzed for Si by this method to provide comparable data.

Intermetallics are generally dissolved in the ammonium sulfate - citric acid electrolyte. The Laves phase could not be detected in these extracts either by X-ray diffraction or energy dispersive analysis. All the particles analyzed by energy dispersive spectroscopy had the composition expected for either gamma prime or a tantalum (Ta)-rich MC. Thus, if it is assumed there was no Laves in the ammonium sulfate - citric acid extracts, their Si concentrations should have been nearly that of the gamma prime alone. The presence of the MC had little effect, since the amount of MC is less than 3 wt% of the extracted gamma prime plus MC and also the MC contains very little Si. Electron microprobe analyses of the alloy with nominal 1-wt% Si confirmed the MC to be essentially TaC.

The Laves phase formed by segregation of Si to the interdendritic areas is essentially the $Mo(Ni,Si)_2$ phase in the Ni-Mo-Si ternary system (refs. 24 and 25). It appears in figures 13 and 14 as a shade of grey intermediate between those of the gamma and gamma-prime phases. It is most readily seen in figure 14(b). Several elongated particles begin at the black void and stretch diagonally across the photomicrograph along a grain boundary.

Finer Laves particles form a necklace on some grain boundaries as can be seen in figures 14(c) and (d), particularly in the Mo X-ray raster scan. The basic composition of these Laves particles was confirmed by electron microprobe analysis.

The Laves phase was identified in X-ray diffraction patterns of the extracted minor phases from the alloys with Si added. Its structure is hexagonal, with $a = 0.47320 \pm 0.00002$ nm and $c = 0.76654 \pm 0.00003$ nm in the alloy with 1.1-wt% Si.

Other heat treatments. - The heat treatment which was most beneficial to the stress-rupture life and ductility of all the alloys, 1200° C for 2 hours plus 900° C for 10 hours, had only subtle effects on their microstructure. Figure 15 shows the alloy with 1.1-wt% Si after this heat treatment. There has been only slight dissolution of the massive gamma-prime nodules. The only change which would be judged beneficial is the refinement in the gamma-prime distribution in the vicinity of the grain boundaries. The Laves phase appears to have been only somewhat coarsened.

The effects of this heat treatment were generally the same on the alloy with 0.6-wt% Si, but any effects on the alloy without the Si added were not obvious. Possibly the 1200° C solution treatment allowed precipitation of more fine gamma prime in the matrix between the larger cuboidal precipitates during the aging treatment. If so, this could not be resolved in the scanning electron microscope.

The heat treatments employing the higher solution temperatures of 1230° and 1260° C did dissolve more of the massive gamma-prime nodules in the alloys with Si added. They also provided the same zone of refined gamma-prime distribution in the vicinity of the grain boundaries seen in figure 15. However, as the solution temperature was increased a necklace of coarse gamma prime developed immediately at the grain boundaries. The beginnings of this necklace formation can be seen in the alloy with 1.1-wt% Si after the standard 1080° C-plus-aging heat treatment (fig. 14(a)) and after the 1200° C-plus-aging heat treatment (fig. 15). This necklace also formed in the B-1900 control specimens after the 1230° and 1260° C solution treatments, but it did not reach the same degree of continuity as in the alloys with Si added.

The highest-temperature solution treatments also produced a thick film of gamma prime around the original MC carbides, probably indicating they were undergoing decomposition. This film occurred in the alloys with and without Si added. Finally, in the 1.1-wt%-Si alloy, definite incipient melting around the massive gamma-prime nodules occurred at 1260° C and possible at 1230° C also.

All these factors were likely to have been responsible for the general decrease in rupture life with increased solution temperature above 1200° C for the alloys with Si added. Why the rupture life of the B-1900 without Si added continually increased with increasing solution temperature was not obvious from examination of the microstructures.

Phase stability. - X-ray diffraction studies of the electrolytically extracted minor phases from alloys exposed for 1500 hours at 870° C showed that no sigma-related phases had formed. Only the expected reactions of the MC to form M_6C and some $M_{23}C_6$ carbides were observed (refs. 22 and 26). The Laves phase was still present as a large percentage of the minor phases in the alloys with Si added.

CONCLUDING REMARKS

The markedly beneficial effect of Si additions on the oxidation resistance of B-1900 has been confirmed by cyclic heating in high-velocity gas. B-1900 + 0.6-wt% Si is as oxidation resistant as aluminide-coated B-1900. Also, it appears that B-1900 + 0.6-wt% Si given a heat treatment of 1200° C for 4 hours plus 900° C for 10 hours has stress-rupture properties not greatly different from those of B-1900 given the standard heat treatment.

These results are felt to be very promising in that an inherently oxidation-resistant alloy not requiring a coating for additional oxidation protection could offer cost savings and increased reliability from oxidation damage. However, sulfidation and/or thermal fatigue may well limit the life of turbine blades cast from B-1900 + 0.6-wt% Si as compared with aluminide-coated B-1900 blades. Further work would be necessary to develop a viable alloy to operate without a coating.

However, allowing higher Si concentrations than currently specified in nickel-base superalloys could be very useful even if a coating were necessary to increase resistance to sulfidation and thermal fatigue. Some advanced engine designs anticipate metal temperatures high enough that oxidation could be a problem in internal blade cooling passages, which are difficult to coat. Improved oxidation resistance of the base material would certainly be beneficial in such an application.

Since it has been shown that Si greatly improves the oxidation resistance of gamma prime (refs. 1 and 2) and of a high-fraction-gamma-prime superalloy, B-1900, there is reason to expect this effect might occur in other advanced Ni-base superalloys. Thus, it seems that higher Si concentrations than usually specified should be investigated in future development of Ni-base superalloys.

SUMMARY OF RESULTS

Cast specimens of the nickel-base superalloy B-1900 with nominal additions of 0-, 0.5-, and 1-wt% silicon were tested together with aluminide-coated B-1900 specimens for oxidation and sulfidation resistance during exposure to a Mach 1 burner exhaust. The alloys were also tested in tension and stress rupture after various heat treatments, and extensively studied metallographically. The major results of this study are as follows:

1. The addition of small concentrations of silicon to alloy B-1900 markedly improved resistance to oxidation during cyclic heating in static air and high-velocity gas.

2. A silicon concentration of 0.6 wt% was nearly as effective as 1.3 wt% in improving cyclic oxidation resistance.

3. The high-gas-velocity oxidation resistance of B-1900 with 0.6-wt% silicon was equivalent to that of B-1900 with a commercial aluminide coating.

4. The improvement in oxidation resistance was associated with an increased fraction of Al_2O_3 in the scale, which was also thinner and more resistant to spalling. This appeared to happen because Si reduced the rates of formation of the less protective oxides, NiO and spinel, which compete with Al_2O_3 formation.

5. The onset of thermal fatigue cracking in the cyclic high-gas-velocity oxidation test appeared to be delayed by the silicon additions, but the aluminide-coated specimens were definitely superior to all the uncoated alloys.

6. The silicon additions improved sulfidation resistance, but the aluminide-coated specimens were definitely superior.

7. The addition of silicon reduced 1000° C rupture strength for specimens given the standard heat treatment of 1080° C for 4 hours plus 900° C for 10 hours to simulate a commercial aluminide-coating cycle.

8. A heat treatment of 1200° C for 4 hours followed by 900° C for 10 hours improved the 1000° C rupture strength of all three alloys studied. The rupture strength of the alloy with 0.6-wt% silicon was equivalent to that of unmodified B-1900 given the standard heat treatment.

9. None of the heat treatments applied increased the 1000° C rupture strength of the 1.1-wt% Si alloy to that of the unmodified B-1900.

10. Silicon additions to B-1900 cause much of the gamma prime to precipitate as large nodules during solidification.

11. A Laves phase, essentially $Mo(Ni,Si)_2$, appeared in the silicon-modified alloys.

Lewis Research Center,
National Aeronautics and Space Administration,
Cleveland, Ohio, March 5, 1975,
505-01.

REFERENCES

1. Santoro, Gilbert J.; Deadmore, Daniel L.; and Lowell, Carl E.: Oxidation of Alloys in the Nickel-Aluminum System with Third-Element Additions of Chromium, Silicon, and Titanium at 1100° C. NASA TN D-6414, 1971.

2. Lowell, Carl E.; and Santoro, Gilbert J.: The 1200° C Cyclic Oxidation Behavior of Two Nickel-Aluminum Alloys (Ni_3Al and NiAl) with Additions of Chromium, Silicon, and Titanium. NASA TN D-6838, 1972.

3. Lowell, Carl E.; and Miner, R. V., Jr.: Improvement in the Cyclic Oxidation of the Nickel-Base Superalloy B-1900 by the Addition of One Percent Silicon. NASA TM X-68191, 1973.

4. High Temperature, High Strength Nickel Base Alloys. Rev. ed., International Nickel Co., Inc., 1968.

5. Barrett, C. A.; and Evans, E B.: Cyclic Oxidation Evaluation - Approaching Application Conditions. Presented at American Ceramic Society, Annual Meeting and Exposition, 75th, Cincinnati, Oh., Apr. 29 - May 3, 1973.

6. Johnston, James R.; and Ashbrook, Richard L.: Oxidation and Thermal Fatigue Cracking of Nickel- and Cobalt-Base Alloys in a High Velocity Gas Stream. NASA TN D-5376, 1969.

7. Donachie, Matthew J., Jr.; and Kriege, Owen H.: Phase Extraction and Analysis in Superalloys - Summary of Investigations by ASTM Committee E-4, Task Group 1. J. Materials, vol. 7, no. 3, Sept. 1972, pp. 269-278.

8. Gordon, William A.; and Chapman, Gilbert B.: Quantitative Direct-Current Arc Analysis of Random Compositions of Microgram Residues in Silver Chloride Common Matrix. Spectrochimica Acta, vol. 25B, 1970, pp. 123-137.

9. Garlick, Ralph G.; and Lowell, Carl E.: Alloy Composition Effects on Oxidation Products of VIA, B-1900, 713C, and 738X - A High Temperature Diffractometer Study. NASA TM X-2796, 1973.

10. Gulbransen, Earl A.; and Andrew, Kenneth F.: Oxidation Studies on the Nickel-Chromium and Nickel-Chromium-Aluminum Heater Alloys. J. Electrochem. Soc., vol. 106, no. 11, Nov. 1959, pp. 941-948.

11. Sugiyama, M.; and Nakayama, T.: Effect of Si on High-Temperature Oxide Films in Heat-Resisting Alloys. Nippon Kinzoku Gakkaiski, vol. 24, no. 8, 1960, pp. 541-544.

12. Douglas, D. L.; and Armijo, J. S.: The Effect of Silicon and Manganese on the Oxidation Mechanism of Ni-20Cr. J. Oxid. Metals, vol. 2, no. 2, 1970, pp. 207-231.

13. Lowell, Carl E.: Cyclic and Isothermal Oxidation Behavior on Some Ni-Cr Alloys. J. Oxid. Metals, vol. 7, no. 2, 1973, pp. 95-115.

14. Lustman, B.: The Intermittent Oxidation of Some Nickel-Chromium Base Alloys. Trans. AIME, vol. 188, Aug. 1950, pp. 995-996.

15. Wood, Graham C.: High-Temperature Oxidation of Alloys. J. Oxid. Metals, vol. 2, no. 11, 1970, pp. 11-57.

16. Wood, G. C.: Fundamental Factors Determining The Mode of Scaling of Heat-Resistant Alloys. Werkstoffe u. Korrosion, vol. 22, no. 6, June 1971, pp. 491-503.

17. Saegusa, Fumihiko: The Oxidation Mechanism of Nickel-Silicon Alloy. WVT-6837, Benet Labs., Watervliet Arsenal (AD-683609), 1968.

18. Barrett, Charles A.; and Lowell, Carl E.: Comparison of Isothermal and Cyclic Oxidation Behavior of Twenty-Five Commercial Sheet Alloys at 1150° C. NASA TN D-7615, 1974.

19. Barrett, Charles A.; Santoro, Gilbert J.; and Lowell, Carl E.: Isothermal and Cyclic Oxidation at 1000° and 1100° C of Four Nickel-Base Alloys: NASA-TRW VIA, B-1900, 713C, and 738X. NASA TN D-7484, 1973.

20. Walters, J. J.: Study of the Hot Corrosion of Superalloys. Avco Corp. (AFML-TR-67-297; AD-822779), 1967.

21. Sittner, Miroslav: Segregation of Components in Ternary Nickel-Base Alloys. Z. fur Metallkde., vol. 64, no. 9, Sept. 1973, pp. 635-639.

22. Danesi, W. P.; Donachie, M. J.: and Radavich, J. F.: Phase Reactions in B-1900 Nickel-Base Alloy From 1600° to 1800° F. Trans. ASM, vol. 59, 1966, pp. 505-516.

23. Kriege, Owen H.; and Baris, J. M.: The Chemical Partitioning of Elements in Gamma Prime Separated from Precipitation-Hardened, High-Temperature Nickel-Base Alloys. Trans. ASM, vol. 62, no. 1, Mar. 1969, pp. 195-200.

24. Gladyshevskii, E. I.; and Kuzma, Yu. B.: Crystal Structure of Ternary Phases In the Systems Mo(W)-Fe(Co,Ni)-Si. Zhur. Strukt. Khim., vol. 1, no. 1, May - June 1960, pp. 57-62.

25. Vivkar, Anil V.; and Raman, Aravamudhan: Alloy Chemistry of Sigma (Beta-U)-Related Phases. II. The Characteristics of Delta and Other Sigma-Related Phases in Some Mo-NiX Systems. Z. fur Metallkde., vol. 60, no. 7, July 1969, pp. 594-600.

26. Collins, H. E.: Relative Long-Time Stability of Carbide and Intermetallic Phases in Nickel-Base Superalloys. Trans. ASM, vol. 62, no. 1, Mar. 1969, pp. 82-104.

TABLE I. - CHEMICAL ANALYSIS OF B-1900

MASTER HEATS

Element	Master heat 1	Master heat 2	B-1900 (nominal)[a]
	Concentration, wt %		
Aluminum	6.0	6.2	6.0
Carbon	.094	.12	.10
Cobalt	10.0	10.1	10.0
Chromium	8.0	8.0	8.0
Molybdenum	6.0	6.1	6.0
Tantalum	4.2	4.1	4.0
Titanium	1.1	1.1	1.0
Zirconium	.095	.071	.10
Boron	.020	.015	.015
Iron	.06	.06	------
Sulfur	.007	.006	------
Manganese	< .02	< .02	------
Silicon	< .05	< .05	------
Tungsten	< .05	.07	------
Niobium	< .05	< .05	------
Bismuth	< .00005	< .00003	------
Lead	< .0001	.00007	------
Nickel	Balance	Balance	Balance

[a]Ref. 4

TABLE II. - SILICON ANALYSIS OF ALLOY CASTINGS

Specimen type	Master heat - casting	Aim	Actual
		Silicon concentration, wt %	
Mechanical test specimens	1-7	<0.05	<0.05
	1-8	<.05	<.05
	1-0	.5	.80
	1-2	1.0	1.02
Oxidation specimens, static air and high gas velocity	1-4	<0.05	<0.05
	1-5	.5	.61
	1-6	1.0	1.31
Mechanical test specimens	2-1	<0.05	<0.05
	2-2	.5	.58
	2-3	1.0	1.09

TABLE III. - CYCLIC FURNACE SCHEDULE

Heating	Cooling
Time per cycle, hr	
0.10	0.15
1.0	.67
10.0	.67
100.0	.67

TABLE IV. - STRESS-RUPTURE DATA

Test conditions	Specimen condition	Master heat - casting	Silicon concentration, wt %	Life, hr	Elongation, percent	Reduction of area, percent
1000° C; 152 MN/m^2	Standard heat treatment, 1080° C/4 hr/air cooled + 900° C/10 hr/air cooled	1-7	<0.05	58.6	4.8	5.2
				57.5	5.6	5.6
				65.7	4.0	4.9
		1-8	<0.05	62.7	4.8	4.8
				64.9	4.8	4.9
				70.6	4.8	4.3
		1-0	0.80	33.2	4.0	7.7
				44.1	(b)	7.0
		1-2	1.02	28.4	7.2	7.6
				22.6	6.4	9.7
		2-1	<0.05	65.4	7.2	10.3
				88.0	7.2	9.2
		2-2	0.58	51.2	6.4	8.4
				58.4	(b)	9.1
		2-3	1.09	27.3	(b)	11.9
				30.7	(b)	8.4
		[a]B-1900	<0.25	100	---	----
	1200° C/2 hr/air cooled + 900° C/10 hr/air cooled	2-1	<0.05	83.1	5.6	14.2
				105.5	7.2	10.7
				82.5	6.4	13.2
		2-2	0.58	68.0	(b)	10.2
				77.9	4.8	4.8
		2-3	1.09	52.4	8.8	13.4
				27.3	9.6	15.7
	1230° C/24 hr/air cooled	2-1	<0.05	105.0	(b)	10.3
				99.1	3.2	4.8
		2-2	0.58	42.6	4.0	4.8
				89.0	3.2	4.8
		2-3	1.09	42.9	(b)	17.8
				40.0	8.0	15.2
	1260° C/24 hr/air cooled + 900° C/10 hr/air cooled	2-1	<0.05	116.3	3.2	4.8
				85.5	3.2	4.8
		2-2	0.58	69.0	1.6	3.2
				52.5	2.4	4.0
		2-3	1.09	39.5	(b)	2.0
				24.9	1.6	1.6
760° C; 648 MN/m^2	1200° C/2 hr/air cooled + 900° C/10 hr/air cooled	1-7	<0.05	29.3	1.6	3.6
		1-8		12.1	1.6	3.2
		1-8		108.2	3.2	5.6
		1-0	0.80	10.3	1.6	1.6
				23.3	1.6	1.6
		1-2	1.02	41.4	0.8	1.2
				28.5	2.4	2.4
	Standard heat treatment	[a]B-1900	<0.25	90	---	----

[a]Typical properties of cast test bars given the standard heat treatment (private communication from S. S. Blecherman, Pratt & Whitney Aircraft).

[b]Elongation was not measured when for some reason the broken halves of the specimen would not fit together well.

TABLE V. - TENSILE TEST DATA FOR ALLOYS GIVEN STANDARD HEAT TREATMENT (1080° C/4 HR/AIR COOLED + 900° C/10 HR/AIR COOLED)

Test temperature, °C	Master heat - casting	Silicon concentration, wt %	Yield strength at 0.2 percent offset, MN/m^2	Ultimate tensile strength, MN/m^2	Elongation, percent	Reduction of area, percent
Room	1-7	<0.05	755	818	2.4	5.3
↓	1-8	<.05	772	845	3.6	6.4
	1-0	.80	725	777	2.0	2.9
	1-2	1.02	696	828	1.8	4.0
	[a]B-1900		800	903	8	---
650	1-7	<0.05	763	883	6.3	5.1
↓	1-8	<.05	761	842	2.8	4.3
	1-0	.80	758	784	1.0	1.7
	1-2	1.02	799	864	1.5	2.1
	[a]B-1900		807	910	5	---

[a]Typical properties of cast test bars given the standard heat treatment (private communication from S. S. Blecherman, Pratt & Whitney Aircraft).

TABLE VI. - ANALYSES OF PHASES EXTRACTED ELECTROLYTICALLY FROM B-1900 ALLOYS WITH VARIOUS SILICON CONCENTRATIONS

	Master heat - casting			Kriege and Baris (ref. 23)
	2-1	2-2	2-3	
Alloy silicon concentration,[a] wt %	<0.05	0.49	0.91	----
Minor phases extracted[b]	MC	MC + Laves	MC + Laves	----
Amount of minor phases extracted,[c] wt %	1.5	2.4	3.2	----
Amount of gamma prime plus MC extracted,[d] wt %	64	62	58	----
Amount of gamma prime in alloy, wt %	62	----	----	61.6
Elemental concentrations in gamma prime plus MC,[e] wt %:				
Silicon[a]	0.046	0.46	0.92	----
Aluminum	7.2	6.9	7.1	8.3
Cobalt	6.1	6.2	6.3	6.1
Chromium	2.6	2.5	2.8	2.8
Molybdenum	3.8	3.7	3.9	3.9
Tantalum	5.7	6.2	5.9	6.1
Titanium	1.4	1.4	1.4	1.6
Nickel	73.2	72.6	71.7	71.2

[a]Determined by atomic absorbtion.

[b]X-ray diffraction analysis of material extracted in HCl-methanol.

[c]Determined by extraction in HCl-methanol as per ref. 7.

[d]Determined by extraction in ammonium sulfate - citric acid as per ref. 7.

[e]All elements except Si determined by emission spectrochemical analysis method of ref. 8.

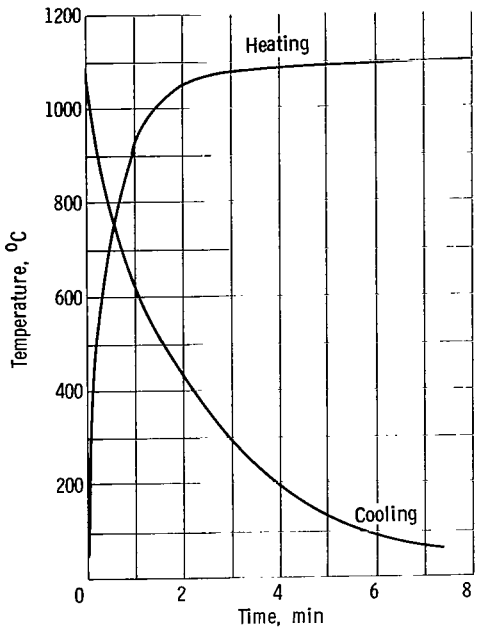

Figure 1. - Heating and cooling curves for B-1900 in cyclic furnace. Sample size, 2.54 cm by 1.27 cm by 0.64 cm.

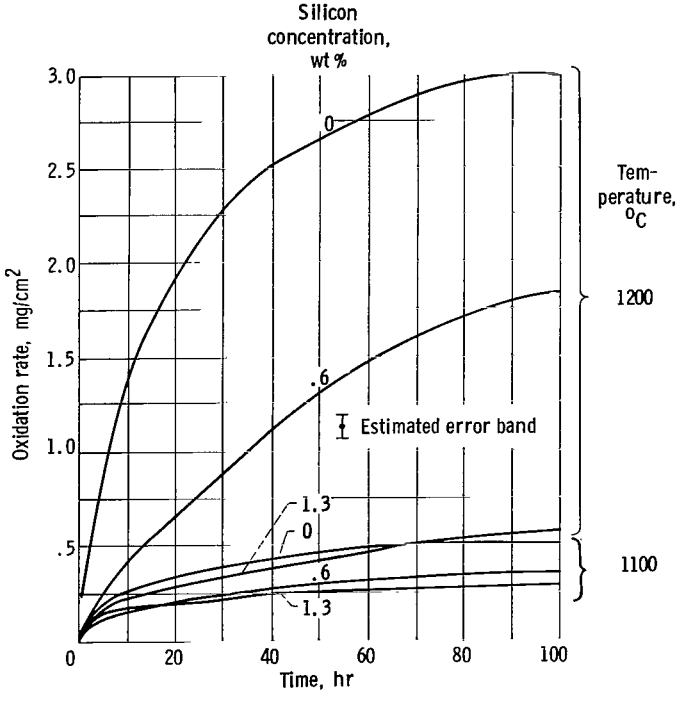

Figure 2. - Effect of temperature and silicon concentration on isothermal oxidation of B-1900.

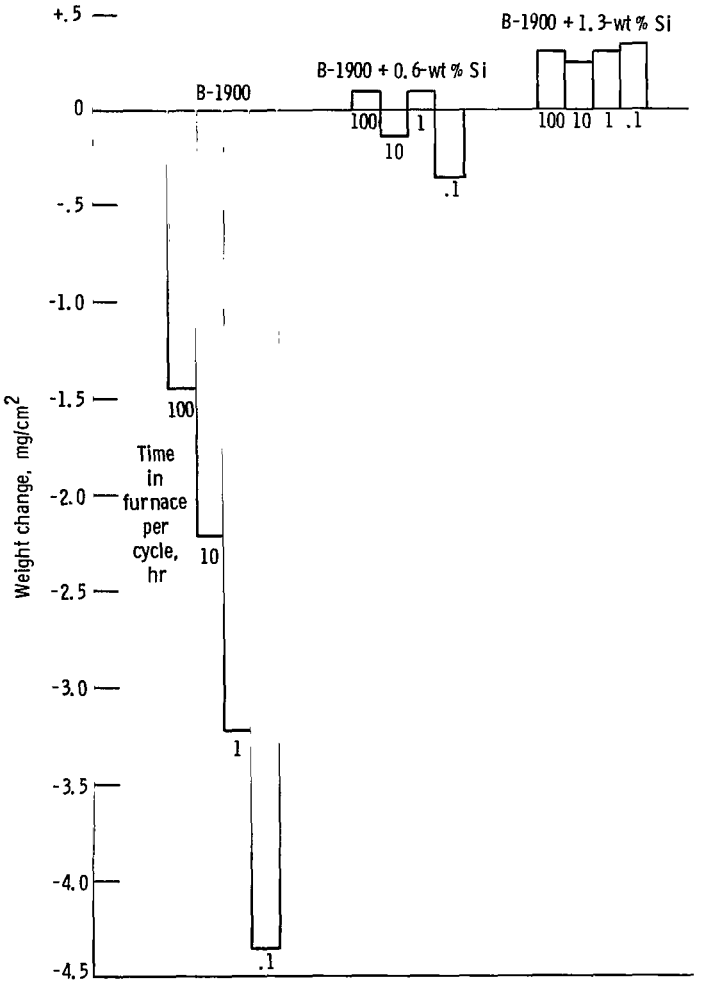

Figure 3. - Effect of cycle period and silicon concentration on cyclic furnace oxidation of B-1900 at 1100° C for 200 hours.

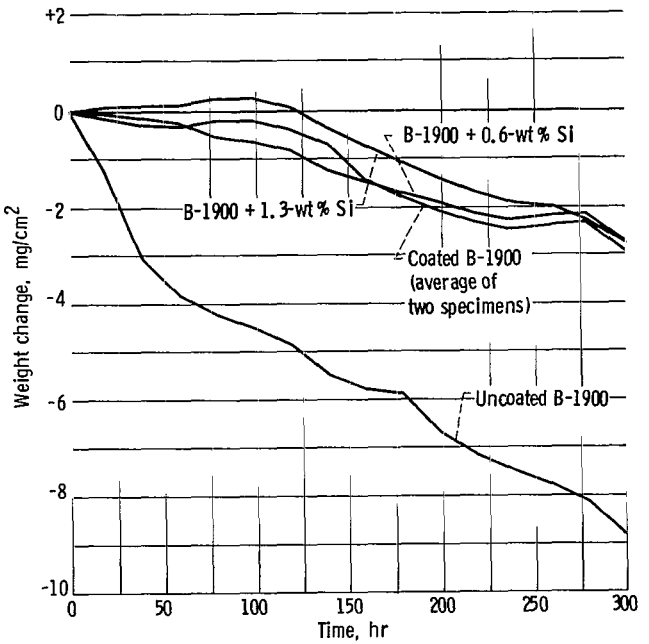

Figure 4. - Effect of silicon concentration on resistance of B-1900 to cyclic oxidation in Mach 1 burner exhaust at 1100° C compared with aluminide-coated B-1900. Cycle time, 1 hr.

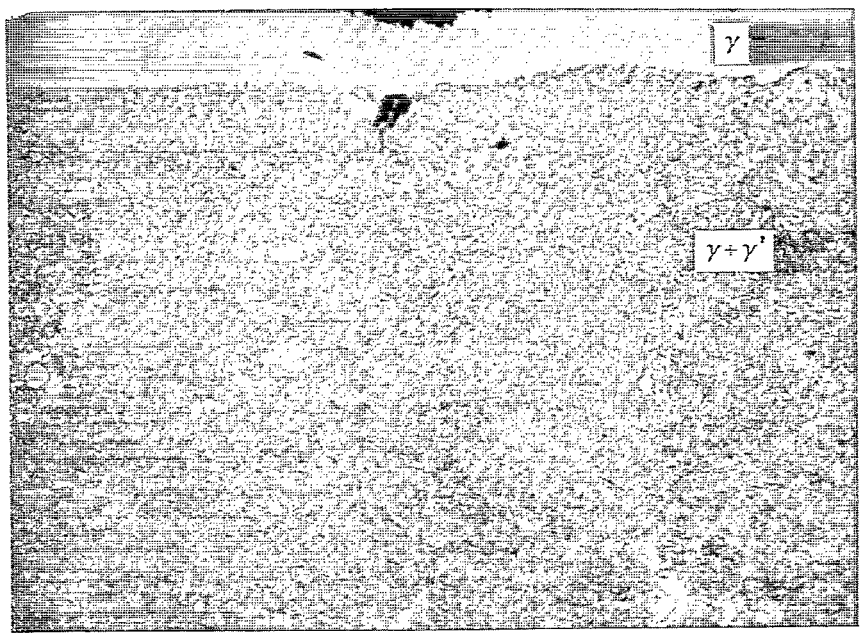

(a) B-1900.

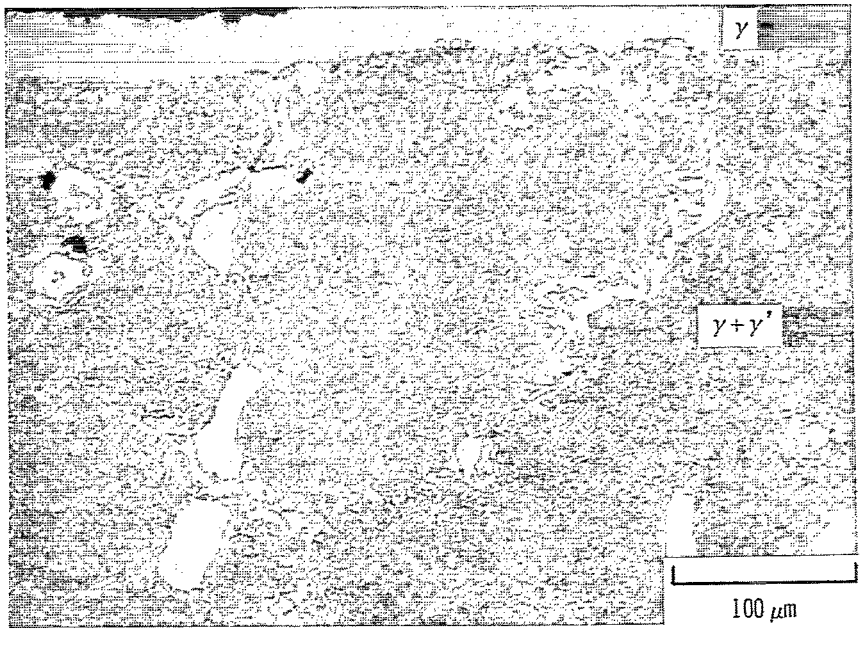

(b) B-1900 + 1.3-wt % silicon.

Figure 5. - Depletion zone after 300 hours in a Mach 1 burner exhaust at 1100° C. Cycle time, 1 hr; etched samples.

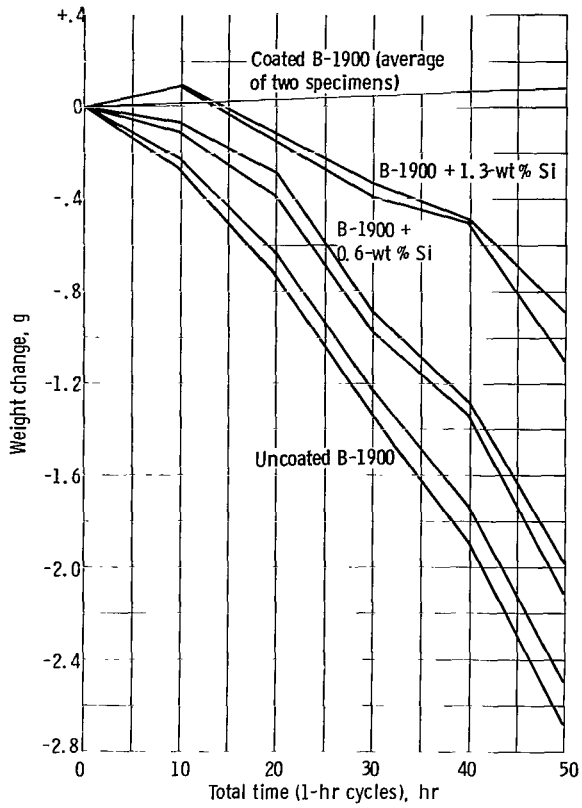

Figure 6. - Effect of silicon concentration on resistance of B-1900 to sulfidation in Mach 1 burner exhaust with 5-ppm salt at 900° C, compared with aluminide-coated B-1900. Cycle time, 1 hr; specimen weight, ~120 g.

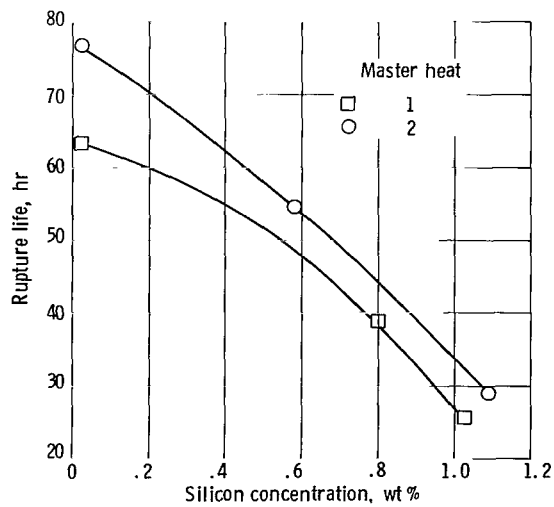

Figure 7. - Effect of silicon concentration on average stress-rupture life at 1000° C and 152 MN/m^2 of alloys given the standard heat treatment (1080° C/4 hr/air cooled + 900° C/10 hr/air cooled).

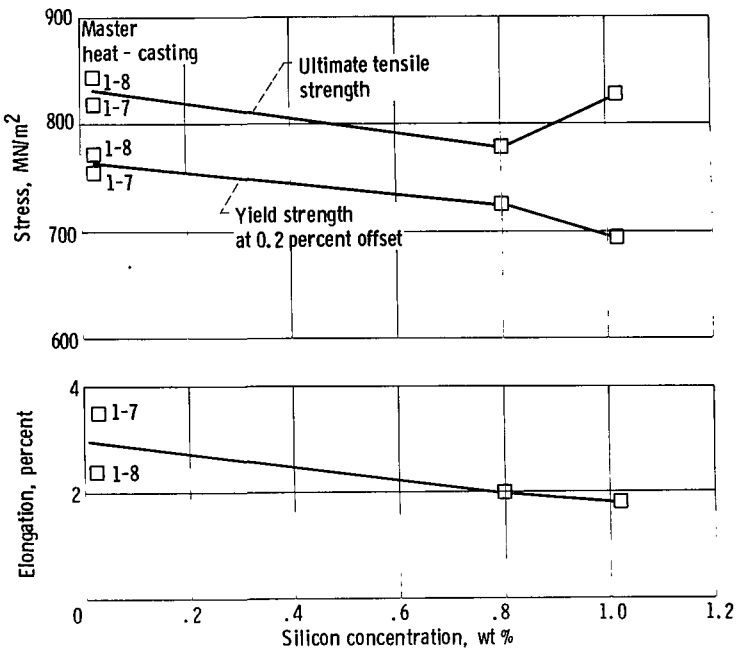

Figure 8. - Effect of silicon concentration on room-temperature tensile properties of alloys from master heat 1 given standard heat treatment (1080° C/4 hr/air cooled + 900° C/10 hr/air cooled).

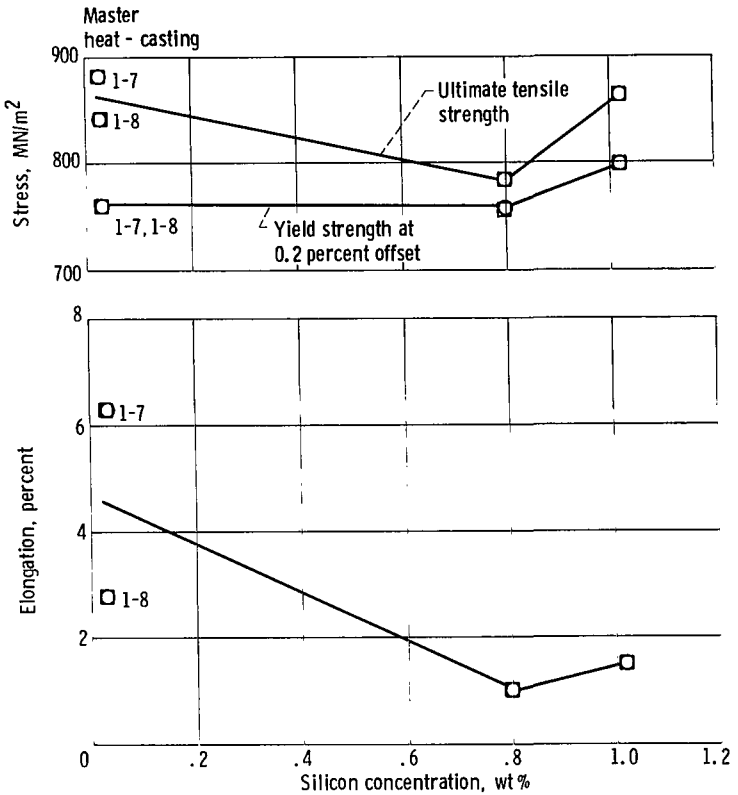

Figure 9. - Effect of silicon concentration on 650° C tensile properties of alloys from master heat 1 given standard heat treatment (1080° C/4 hr/air cooled + 900° C/10 hr/air cooled.

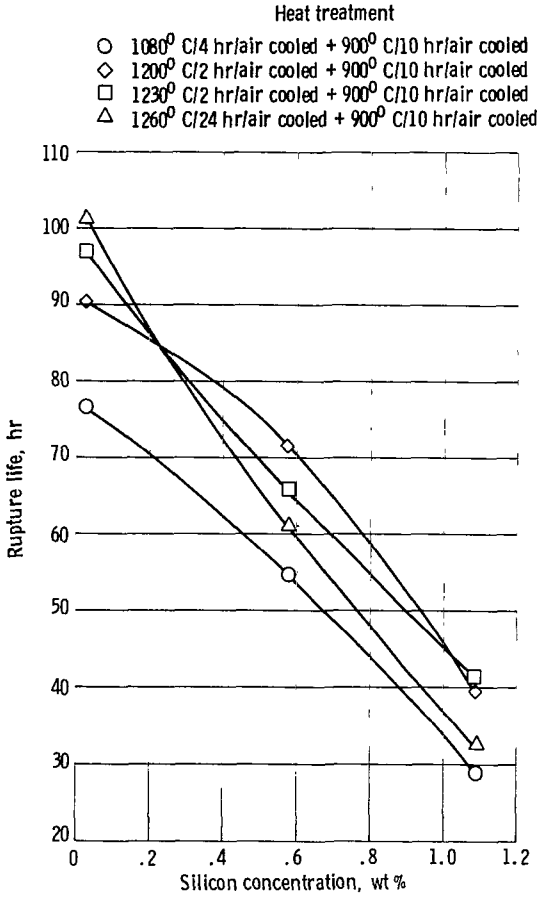

Figure 10. - Effects of various heat treatments on rupture life at 1000° C and 152 MN/m^2 of alloys from master heat 2.

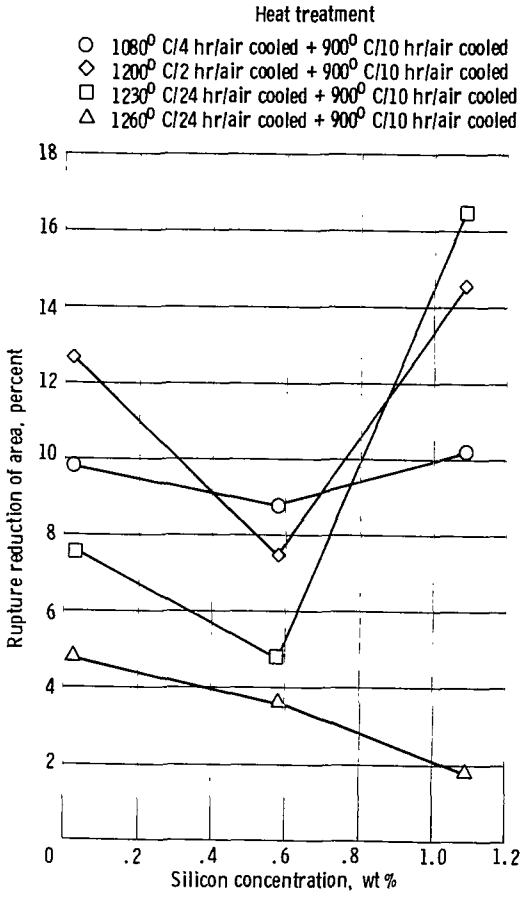

Figure 11. - Effects of various heat treatments on rupture reduction of area of alloys from master heat 2.

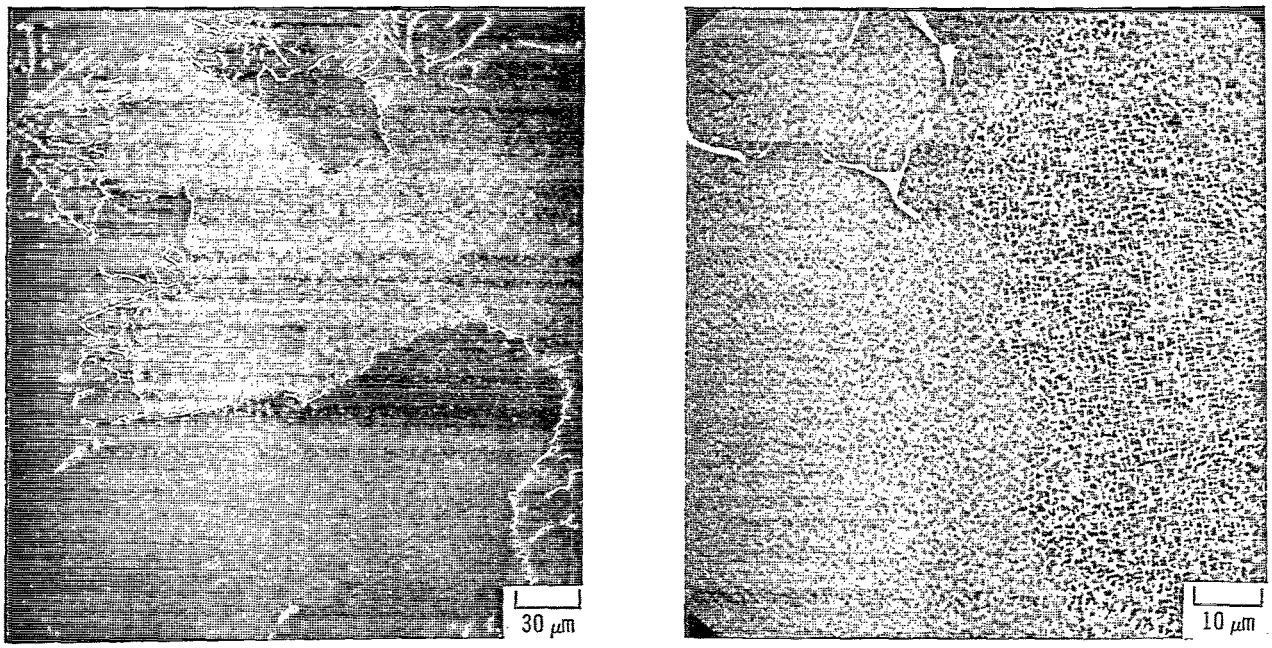

Figure 12. - Scanning electron photomicrographs of unmodified B-1900, casting 1-4, given standard heat treatment (1080° C/4 hr/ air cooled + 900° C/10 hr/air cooled).

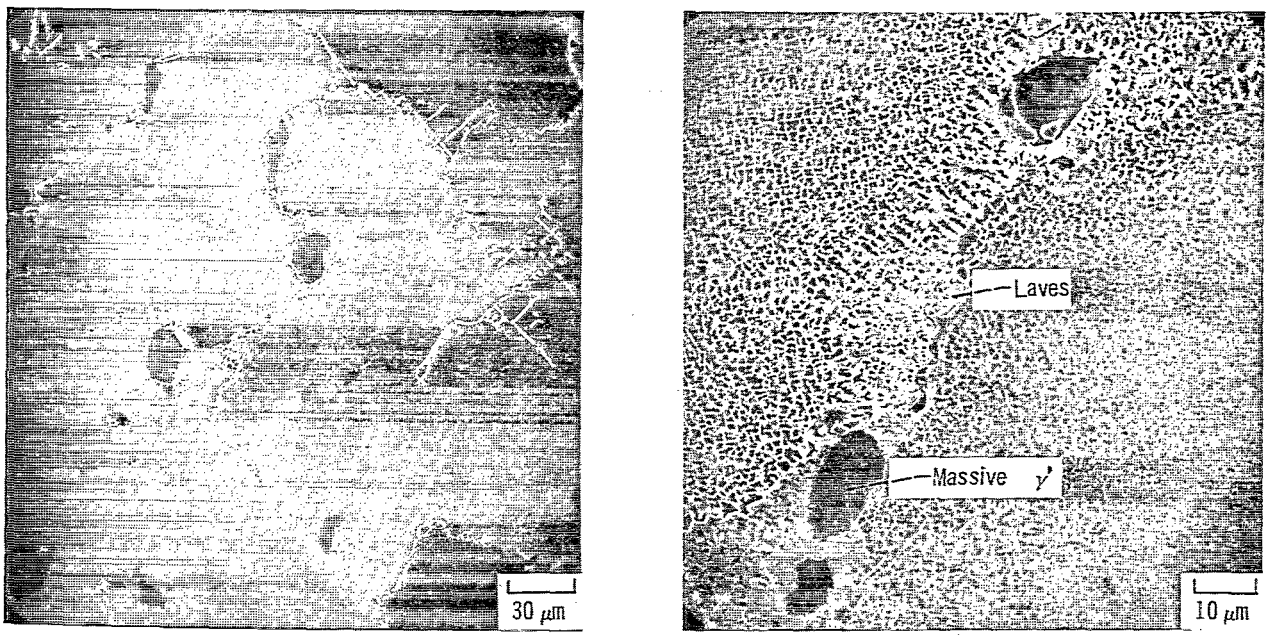

Figure 13. - Scanning electron photomicrographs of B-1900 + 0.6-wt % silicon, casting 1-5, given standard heat treatment (1080° C/4 hr/air cooled + 900° C/10 hr/air cooled).

(a) Secondary electron image showing massive gamma prime.

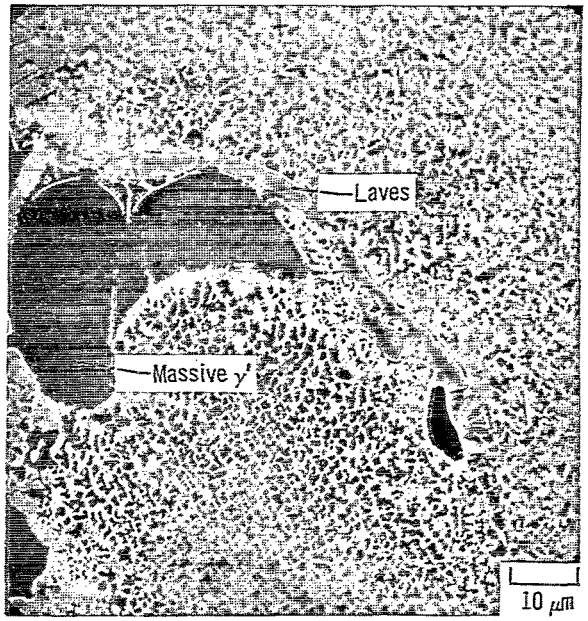

(b) Secondary electron image showing massive gamma-prime and Laves phases.

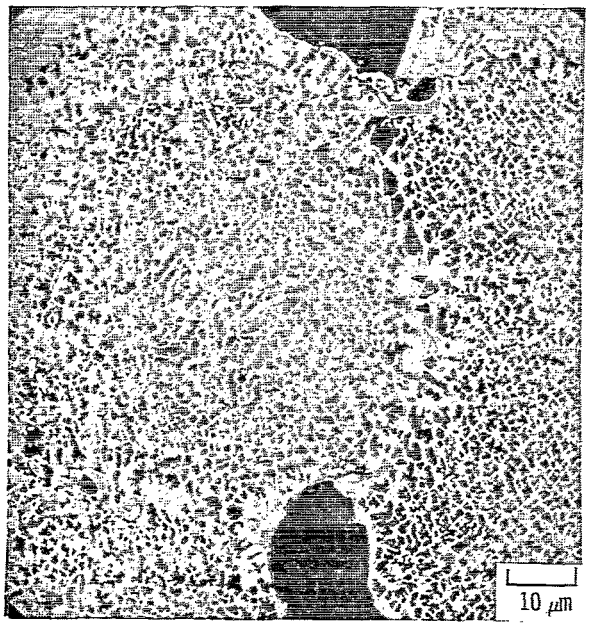

(c) Secondary electron image showing fine-Laves-particle necklace on grain boundary.

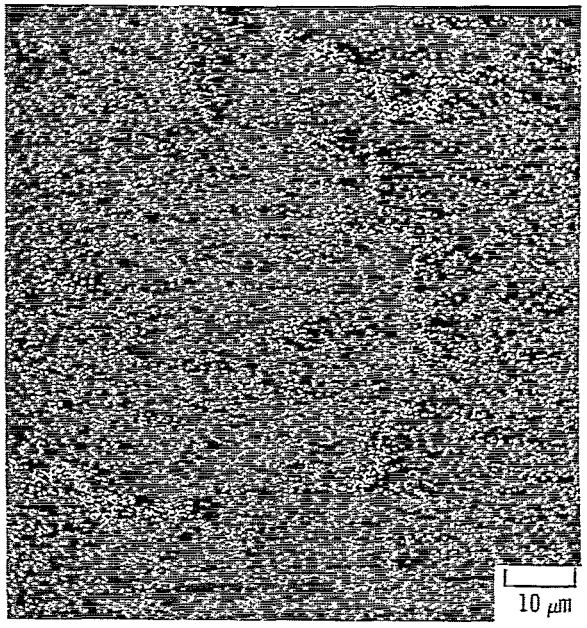

(d) Molybdenum X-ray raster scan showing fine-Laves-particle necklace on grain boundary.

Figure 14. - Scanning electron photomicrographs of B-1900 + 1.3-wt % silicon, casting 1-6, given standard heat treatment (1080° C/4 hr/air cooled + 900° C/10 hr/air cooled).

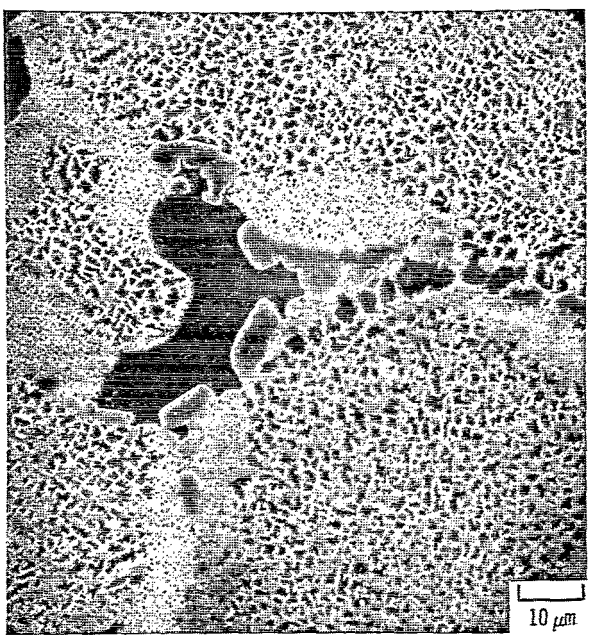

Figure 15. - Scanning electron photomicrograph of B-1900 + 1.1-wt % silicon, casting 2-3, given heat treatment of 1200° C/2 hr/air cooled + 900° C/10 hr/air cooled.

NASA-Langley, 1975 E-8248

"The aeronautical and space activities of the United States shall be conducted so as to contribute . . . to the expansion of human knowledge of phenomena in the atmosphere and space. The Administration shall provide for the widest practicable and appropriate dissemination of information concerning its activities and the results thereof."

—NATIONAL AERONAUTICS AND SPACE ACT OF 1958

NASA SCIENTIFIC AND TECHNICAL PUBLICATIONS

TECHNICAL REPORTS: Scientific and technical information considered important, complete, and a lasting contribution to existing knowledge.

TECHNICAL NOTES: Information less broad in scope but nevertheless of importance as a contribution to existing knowledge.

TECHNICAL MEMORANDUMS: Information receiving limited distribution because of preliminary data, security classification, or other reasons. Also includes conference proceedings with either limited or unlimited distribution.

CONTRACTOR REPORTS: Scientific and technical information generated under a NASA contract or grant and considered an important contribution to existing knowledge.

TECHNICAL TRANSLATIONS: Information published in a foreign language considered to merit NASA distribution in English.

SPECIAL PUBLICATIONS: Information derived from or of value to NASA activities. Publications include final reports of major projects, monographs, data compilations, handbooks, sourcebooks, and special bibliographies.

TECHNOLOGY UTILIZATION PUBLICATIONS: Information on technology used by NASA that may be of particular interest in commercial and other non-aerospace applications. Publications include Tech Briefs, Technology Utilization Reports and Technology Surveys.

Details on the availability of these publications may be obtained from:

SCIENTIFIC AND TECHNICAL INFORMATION OFFICE

NATIONAL AERONAUTICS AND SPACE ADMINISTRATION

Washington, D.C. 20546